Supporting Information

Passive cancer targeting with a viral nanoparticle depends on the stage of tumorigenesis

Juan Zhang[a,c], Wenjing Zhang[a,c], Mengsi Yang[a,c], Weiwei Zhu[a,c], Ming Li[a], Ao Liang[a,c], Hui Zhang[a], Ti Fang[a], Xian-En Zhang[b,c] and Feng Li[a,c]*

[a] State Key Laboratory of Virology, Wuhan Institute of Virology, Center for Biosafety Mega-Science, Chinese Academy of Sciences, Wuhan, 430071, China

[b] National Laboratory of Biomacromolecules, CAS Center for Excellence in Biomacromolecules, Institute of Biophysics, Chinese Academy of Sciences, Beijing, 100101, China

[c] University of Chinese Academy of Sciences, Beijing, 100049, China

*Corresponding author, email: fli@wh.iov.cn

Supplementary Materials and Methods

Materials

Ag_2S QDs coated with polyethylene glycol 10000 (Ag_2S-10K) were purchased from Suzhou NIR-Optics Technologies Co., Ltd. (China). M-SSA-2000 (PEG2K-NHS) was purchased from JenKem Technology Co., Ltd. (Beijing, China).

Preparation of Dps-2K$_{A647}$

The recombinant wild-type Dps was expressed and purified according to a previous procedure.[1] Commercial PEG2K-NHS molecules were added to Dps, corresponding to a Dps monomer: PEG molar ratio of 1:1. The mixture was gently shaken at 25°C for 1 h in the dark, and the reaction mixture was stored at 4°C for 8 h. Free PEG2K-NHS molecules were removed by ultrafiltration using a centrifuge tube with 30 kDa molecular weight cut-off membrane. Then A647 stock solution (5 mg/mL) was added at a Dps monomer: A647 molar ratio of 4:1. After reaction for 2 h at room temperature and storage at 4°C for 12 h, free A647 molecules were removed through dialysis against PBS. PEGylated Dps-2K$_{A647}$ was concentrated to 3 mg/mL (based on Dps protein) for characterization and *in vivo* injection.

H&E staining

At 7 days pi of P22-1K$_{A647}$ (2 mg/mL, 200 μL per mouse), the major organs were collected from the mice after euthanasia and fixed with paraformaldehyde (4%) at 4°C for 24 h. The organs were embedded in paraffin and sliced into 5-μm-thick sections. The organ sections were stained by H&E and observed under a panoramic scanner (3DHISTECH, Budapest, Hungary).

Hematological examination

At 7 days pi of P22-1K$_{A647}$ (2 mg/mL, 200 μL per mouse), blood (100μL) was collected from the mice after euthanasia and anti-coagulated with EDTA. The blood samples were gently mixed and stored at 4°C before being analyzed by an automated Hematology Analyzer (BC-2800vet) from Shenzhen Mindray Bio-Medical Electronics Co., Ltd, China.

Supplementary Results and Discussion

To investigate whether the dependence of tumor targeting by P22 VNPs on tumorigenesis stage also holds for other nanoparticle systems, we performed *in vivo* tumor targeting experiments using another two kinds of nanoparticles, namely a protein nanocage called DNA binding protein from starved cells (Dps) of the bacterium *Listeria innocua*[2] and silver sulfide (Ag_2S) quantum dots (QDs). The Dps protein nanocage has a diameter of 9 nm and was conjugated with polyethylene glycol 2000 and the Alexa Fluor 647 dye (termed Dps-2K$_{A647}$). The Ag_2S QDs have a diameter of *ca*. 6 nm (inorganic core) and were coated with polyethylene glycol 10000 (termed Ag_2S-10K). Ag_2S-10K QDs are characterized by fluorescence emission in the second near-infrared window (NIR-II), which is advantageous to in vivo imaging.[3] TEM observation showed that Dps-2K$_{A647}$ and Ag_2S-10K were uniform (Figure S2a). The hydrodynamic diameters (HD) of Dps-2K$_{A647}$ and Ag_2S-10K were measured by DLS to be 12.93 nm and 17.34 nm, respectively; the zeta potentials of Dps-2K$_{A647}$ and Ag_2S-10K were -19.20 mV and -8.21 mV, respectively (Figure S2b).

At 24 h pi in mice with tumor models of different cancer cell inoculation time, the fluorescence intensity of Dps-2K$_{A647}$ at the tumor location was negatively correlated with the time of tumor growth for both left and right tumors (Figure S3a). There were significant differences in tumor accumulation of Dps-2K$_{A647}$ between the 7-day group and 21-day group for both left and right tumors (Figure S3b). Similar phenomenon was observed for Ag_2S-10K QDs (Figure S3c and S3d). These results indicate that tumorigenesis stage also affects the tumor targeting efficiency of the tiny Dps protein nanocage and Ag_2S QDs.

Supplementary Figures

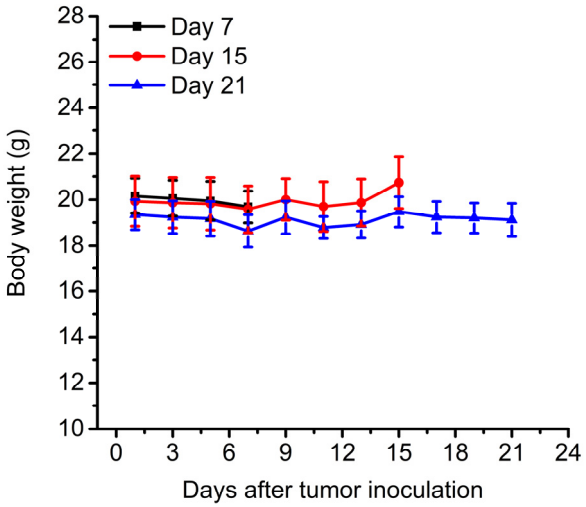

Figure S1. Body weight profiles of the mice from the 7-day, 15-day, and 21-day groups after tumor inoculation. Results are presented as the mean ± SD (n = 4-5).

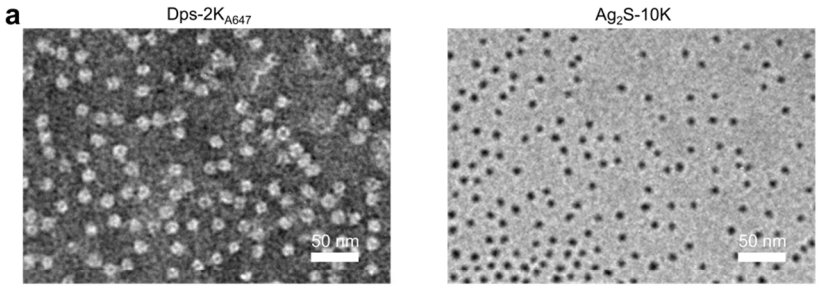

b

	Hydrodynamic diameter (nm)	Zeta potential (mV)
Dps-2K$_{A647}$	12.93±1.07	-19.20±3.17
Ag$_2$S-10K	17.34±1.43	-8.21±0.83

Figure S2. Characterization of Dps-2K$_{A647}$ and Ag_2S-10K nanoparticles. (**a**) TEM images. Scale bars: 50 nm. (**b**) Measurement of hydrodynamic diameter and zeta potential. Results are presented as the mean ± SD (n = 3).

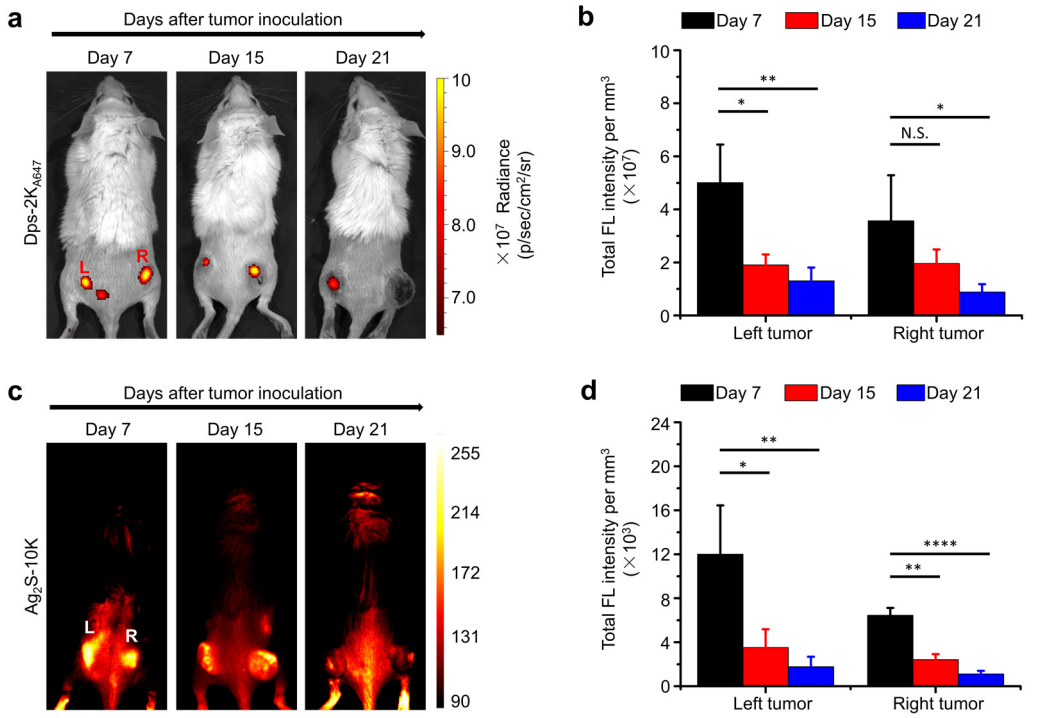

Figure S3. *In vivo* evaluation of tumor targeting efficiency after intravenous injection of Dps-2K$_{A647}$ or Ag_2S-10K nanoparticles in mice inoculated with CT26 colorectal cancer cells for 7, 15, or 21 days. (**a**) *In vivo* fluorescence imaging of Dps-2K$_{A647}$-injected mice. Images were taken at 24 h pi of Dps-2K$_{A647}$. (**b**) Fluorescence quantification of right and left side tumors from Dps-2K$_{A647}$-injected mice at 24 h pi. (**c**) *In vivo* fluorescence imaging of Ag_2S-10K-injected mice. Images were taken at 24 h pi of Ag_2S-10K. (**d**) Fluorescence quantification of right and left side tumors from Ag_2S-10K-injected mice at 24 h pi. Results are presented as the mean ± SD (n = 3-5).

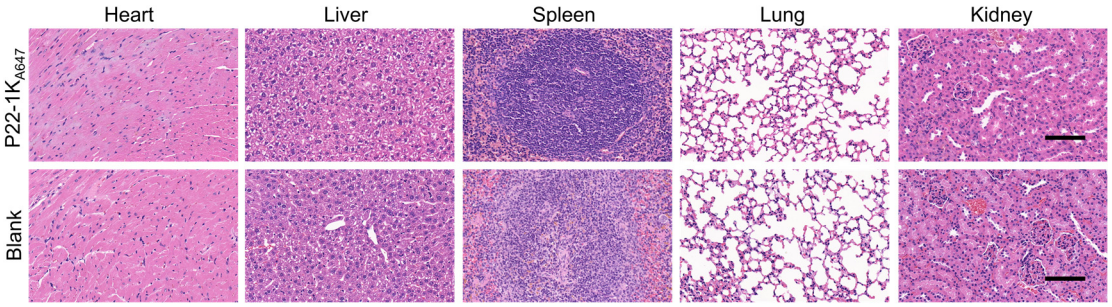

Figure S4. Representative images of the major organ sections stained by hematoxylin and eosin (H&E) at 7 days pi of P22-1K$_{A647}$. Scale bars: 100 μm.

Table S1. Blood cell analysis at 7 days pi of P22-1K_{A647}. Results are presented as the mean ± SD (n = 3).

Parameters	Abbreviation	Mean	SD	Unit	Reference range
White blood cell counts	WBC	5.93	1.76	10^9/L	0.8-6.8
Lymphocytes counts	Lymph	4.67	1.10	10^9/L	0.7-5.7
Monocyte counts	Mon	0.17	0.15	10^9/L	0.0-0.3
Granulocyte counts	Gran	1.10	0.52	10^9/L	0.1-1.8
Lymphocytes Percentage	Lymph%	79.73	6.03	%	55.8-90.6
Monocyte Percentage	Mon%	3.00	1.22	%	1.8-6.0
Granulocyte Percentage	Gran%	17.27	4.82	%	8.6-38.9
Red blood cell	RBC	8.71	1.84	10^{12}/L	6.36-9.42
Hemoglobin	HGB	143.00	38.63	g/L	110-143
Hematokrit	HCT	43.53	10.34	%	34.6-44.6
Mean corpuscular volume	MCV	49.90	1.87	fL	48.2-58.3
Mean cell hemoglobin	MCH	16.27	0.93	pg	15.8-19
Mean cell hemoglobin concentration	MCHC	326.00	14.73	g/L	302-353
Red blood cell distribution width	RDW	13.53	1.50	%	13-17
Platelet counts	PLT	543.00	270.27	10^9/L	450-1590
Mean platelet volume	MPV	6.10	0.61	fL	3.8-6.0

Reference

1. T. Fang, W. Zhu, C. Li, F. Zhang, D. Gao, Z. P. Zhang, A. Liang, X. E. Zhang and F. Li, *Small*, 2019, **15**, 1904838.
2. M. Su, S. Cavallo, S. Stefanini, E. Chiancone and N. D. Chasteen, *Biochemistry*, 2005, **44**, 5572-5578.
3. G. Hong, J. T. Robinson, Y. Zhang, S. Diao, A. L. Antaris, Q. Wang and H. Dai, *Angew. Chem. Int. Ed.*, 2012, **51**, 9818-9821.